



Contents lists available at ScienceDirect

Physics Letters A

www.elsevier.com/locate/pla



## Collective temporal coherence for subthreshold signal encoding on a stochastic small-world Hodgkin–Huxley neuronal network

Mahmut Ozer<sup>a,c,\*</sup>, Muhammet Uzuntarla<sup>a</sup>, Temel Kayikcioglu<sup>b</sup>, Lyle J. Graham<sup>c</sup>

<sup>a</sup> Zonguldak Karaelmas University, Engineering Faculty, Department of Electrical and Electronics Engineering, 67100 Zonguldak, Turkey

<sup>b</sup> Karadeniz Technical University, Department of Electrical and Electronics Engineering, Trabzon, Turkey

<sup>c</sup> Laboratory of Neurophysics and Physiology, UMR 8119 CNRS, Université Paris Descartes, 45 rue des Saint-Peres, 75006 Paris, France

### ARTICLE INFO

#### Article history:

Received 28 July 2008

Received in revised form 2 September 2008

Accepted 3 September 2008

Communicated by R. Wu

#### PACS:

05.40.-a

87.16.-b

87.18.Bb

87.18.Sn

#### Keywords:

Neurons

Stochastic process

Temporal coherence

Complex networks

### ABSTRACT

We study the collective temporal coherence of a small-world network of coupled stochastic Hodgkin–Huxley neurons. Previous reports have shown that network coherence in response to a subthreshold periodic stimulus, thus subthreshold signal encoding, is maximal for a specific range of the fraction of randomly added shortcuts relative to all possible shortcuts,  $p$ , added to an initially locally connected network. We investigated this behavior further as a function of channel noise, stimulus frequency and coupling strength. We show that temporal coherence peaks when the frequency of the external stimulus matches that of the intrinsic subthreshold oscillations. We also find that large values of the channel noise, corresponding to small cell sizes, increases coherence for optimal values of the stimulus frequency and the topology parameter  $p$ . For smaller values of the channel noise, thus larger cell sizes, network coherence becomes insensitive to these parameters. Finally, the degree of coupling between neurons in the network modulates the sensitivity of coherence to topology, such that for stronger coupling the peak coherence is achieved with fewer added short cuts.

© 2008 Published by Elsevier B.V.

### 1. Introduction

The dynamics of complex networks has received considerable attention in recent years and arises in many fields of science [1–5]. In their study of network dynamics and network topology, Watts and Strogatz [6] defined a new class of networks, called small-world (SW) networks, that combine high clustering, thus local structure, with scattered long range connections that give a small average connection distance. SW networks can be described by a set of vertices, and the edges representing their interactions, for example starting from a ring lattice with connections between neighbors. In the model of Watts and Strogatz the final topology is achieved by rewiring each edge at random with a probability  $p$ , resulting in either a regular ( $p = 0$ ), disordered ( $p = 1$ ) or SW networks ( $0 < p < 1$ ) [6]. The Newman–Watts model is a variation of the Watts–Strogatz model [6], where “long-range” random shortcuts are added between pairs of non-adjacent-vertices chosen

at random, while maintaining the original edges of the underlying ring [7–9]. In comparison to the Watts–Strogatz SW model [6] where edges are rewired, thus maintaining a fixed number of connections, in this model the new long-range edges increase the total number of connections from that of the original network [7–9].

SW networks have been shown to enhance signal propagation speed, computational power, and synchronizability [6], and are an attractive model for the organization of both anatomical and functional networks in the brain because this architecture can support both local and distributed information processing [10]. For this reason SW networks have been widely used to understand how neuronal circuitry generates complex patterns of activity. Lago-Fernandez et al. [11] investigated the role of different connectivity regimes on the dynamics of a network of Hodgkin–Huxley (HH) neurons, and showed that SW topologies have dynamics characteristic of both regular and random networks: A fast system response, which is characteristic of random topologies, and coherent oscillations, which are more evident in regular topologies. Kwon and Moon [12] have found that increasing the randomness of the topology of an HH neuron network leads to an enhancement of the network's temporal coherence and spatial synchronization. Simard et al. [13] showed that SW connectivity reduces both learning error and learning time, compared to networks with either completely

\* Corresponding author at: Zonguldak Karaelmas University, Engineering Faculty, Department of Electrical and Electronics Engineering, 67100 Zonguldak, Turkey. Tel.: +90 372 257 5446; fax: +90 372 257 4023.

E-mail address: mahmutozer2002@yahoo.com (M. Ozer).

1 regular or completely random connectivity. Using the Newman–  
2 Watts model, Gong et al. [14] studied the dynamics of an SW  
3 network of stochastic HH neurons. They found that at a given fixed  
4 coupling strength and channel noise, the temporal coherence and  
5 spatial synchronization of the network in response to subthreshold  
6 periodic forcing was maximal for an optimal fraction of random  
7 shortcuts  $p$ .

8 Our aim in this Letter is to extend the analysis of Gong et al.  
9 [14] on the same network model. Due to the importance of fre-  
10 quency tuning in weak signal detection and transduction [15–19],  
11 we first investigated how the relationship between network co-  
12 herence and network topology depends on the stimulus frequency,  
13 with the same coupling and noise parameters used by Gong et  
14 al. [14]. We then measured explicitly the relationship between the  
15 response timing and the stimulus, in terms of phase-locking and  
16 cycle-skipping, as a function of network topology for a single neu-  
17 ron and the network with different values of  $p$ . Finally, we inves-  
18 tigated how the strength of coupling and noise affected network  
19 coherence, as functions of  $p$  and, in the case of noise, also as a  
20 function of stimulus frequency.

21  
22 **2. Methods**

23  
24 The stochastic channel models and the network model studied  
25 here follow that used by Gong et al. [14]. The time evolution of  
26 the membrane potential for the coupled, identical HH neurons on  
27 a network is given as follows:

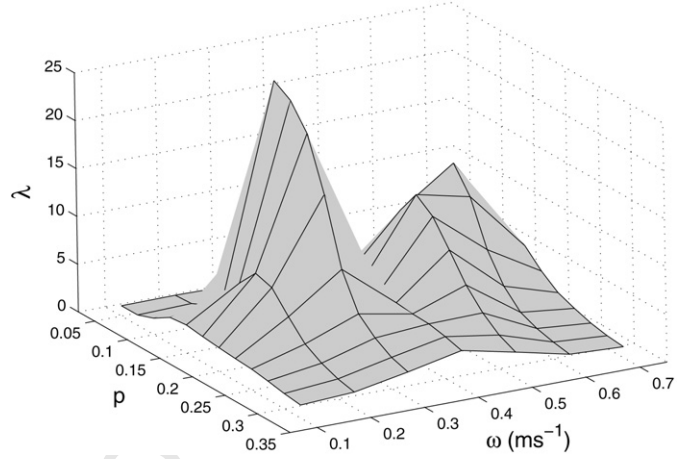
28  
29 
$$C_m \frac{dV_i}{dt} = -g_{Na} m_i^3 h_i (V_i - V_{Na})$$
  
30  
31 
$$- g_K n_i^4 (V_i - V_K) - g_L (V_i - V_L)$$
  
32  
33 
$$+ I_{ext}(t) + \sum_j \varepsilon_{ij} (V_j - V_i), \quad (1)$$
  
34

35 where  $1 \leq i \leq N$ .  $N$  is the number of neurons on the net-  
36 work.  $V_i$  denotes the membrane potential of neuron  $i$ , and  $C_m =$   
37  $1 \mu\text{F cm}^{-2}$  is the membrane capacity.  $g_{Na} = 120 \text{ mS cm}^{-2}$  and  $g_K =$   
38  $36 \text{ mS cm}^{-2}$  are the maximal sodium and potassium conductances,  
39 respectively. In the model, the leakage conductance is assumed to  
40 be constant,  $g_L = 0.3 \text{ mS cm}^{-2}$ .  $V_{Na} = 50 \text{ mV}$ ,  $V_K = -77 \text{ mV}$  and  
41  $V_L = -54.4 \text{ mV}$  are the reversal potentials for the sodium, potas-  
42 sium and leakage channels, respectively.  $I_{ext}(t) = A \sin(\omega t)$  denotes  
43 externally applied sinusoidal stimulus, where  $A$  denotes the am-  
44 plitude of the sinusoidal forcing current, which is set to  $1 \mu\text{A/cm}^2$ ,  
45 and  $\omega$  is angular frequency of the current.  $\varepsilon_{ij}$  denotes the coupling  
46 strength between two neurons  $i$  and  $j$ , respectively. If neurons  $i$   
47 and  $j$  are connected, we set the coupling strength to a constant  
48 value of  $\varepsilon_{ij} = \varepsilon$ , otherwise  $\varepsilon_{ij} = 0$ .  $m_i$  and  $h_i$  denote activation  
49 and inactivation variables for the sodium channel of neuron  $i$ , respec-  
50 tively. The potassium channel includes an activation variable,  $n_i$ .

51 In the HH model, activation and inactivation gating variables,  
52  $m_i$ ,  $n_i$  and  $h_i$  change over time in response to the membrane po-  
53 tential following first-order differential equations within the limit  
54 of very large cell membrane area [20]. However, when the popula-  
55 tion of ion channels is finite, stochastic dynamics of voltage-gated  
56 ion channels can have significant implications on the dynamic be-  
57 havior of neurons [21–26]. Stochastic gating variable dynamics are  
58 described with a Langevin generalization [27]:

59  
60 
$$\frac{dx_i}{dt} = \alpha_x (1 - x_i) - \beta_x x_i + \xi_{x_i}(t), \quad x_i = m_i, n_i, h_i, \quad (2)$$
  
61

62 where  $\alpha_x$  and  $\beta_x$  are rate functions for the gating variable  $x_i$ . The  
63 probabilistic nature of the channels appears as a noise source in  
64 Eq. (2),  $\xi_{x_i}(t)$ , which is an independent zero mean Gaussian white  
65 noise source whose autocorrelation function is given as follows  
66 [27–31]:



67  
68  
69  
70  
71  
72  
73  
74  
75  
76  
77  
78  
79  
80  
81  
82  
83  
84 **Fig. 1.** Dependence of collective temporal coherence  $\lambda$  of the random network on  
85 the subthreshold stimulus frequency  $\omega$  and the fraction of random shortcuts  $p$  ( $S =$   
86  $6 \mu\text{m}^2$ ,  $\varepsilon = 0.1$ ,  $A = 1 \mu\text{A/cm}^2$ ).

87  
88 
$$\langle \xi_m(t) \xi_m(t') \rangle = \frac{2\alpha_m \beta_m}{N_{Na}(\alpha_m + \beta_m)} \delta(t - t'), \quad (3)$$
  
89

90  
91 
$$\langle \xi_h(t) \xi_h(t') \rangle = \frac{2\alpha_h \beta_h}{N_{Na}(\alpha_h + \beta_h)} \delta(t - t'), \quad (4)$$
  
92

93  
94 
$$\langle \xi_n(t) \xi_n(t') \rangle = \frac{2\alpha_n \beta_n}{N_K(\alpha_n + \beta_n)} \delta(t - t'), \quad (5)$$
  
95

96 where  $N_{Na}$  and  $N_K$  denotes total number of sodium and potas-  
97 sium channels, respectively. Channel numbers are calculated by  
98  $N_{Na} = \rho_{Na} S$ ,  $N_K = \rho_K S$ , where  $\rho_{Na} = 60 \mu\text{m}^{-2}$  and  $\rho_K = 18 \mu\text{m}^{-2}$   
99 are the sodium and potassium channel densities, respectively, and  
100 represents membrane cell area.

101 The network is comprised of identical coupled HH neurons,  
102 with a size set to  $N = 60$ . We start with a regular ring, where each  
103 neuron is connected to two nearest neighbors, and then add new  
104 edges with a probability  $p$ , i.e., the number of added shortcuts,  $M$ ,  
105 divided by the number of all possible connections [14,32]:

106  
107 
$$p = \frac{M}{N(N-1)/2}. \quad (6)$$
  
108

109 Thus, starting from the original ring, we make a random draw of  
110 two neurons and make a connection between them if none existed  
111 previously, repeating the process until a total of  $M$  new connec-  
112 tions have been added. In the results presented below, for any  
113 given set of the remaining network parameters (input, noise level,  
114 coupling strength), quantitative results were pooled from simula-  
115 tions of ten realizations of the network for any given value of  $p$   
116 (thus  $M$ ).  
117

118 Following Gong et al. [14], we measured the collective temporal  
119 behavior of the network by first calculating the average membrane  
120 potential,  $V_{ave}(t) = \frac{1}{N} \sum_{i=1}^N V_i(t)$ , corresponding to the mean field  
121 of the random network, and then quantifying the network co-  
122 herence by the inverse of the coefficient of variation (CV) of the  
123 inter-spike intervals (ISIs):

124  
125 
$$\lambda = \frac{1}{CV} = \frac{\langle ISI \rangle}{\sigma_{ISI}} = \frac{\langle T \rangle}{\sqrt{\langle T^2 \rangle - \langle T \rangle^2}}, \quad (7)$$
  
126  
127

128 where “spike” times were defined by the upward crossing of the  
129 averaged membrane potentials past a detection threshold of  $0 \text{ mV}$   
130 (referred to below as “network spikes”), and  $\langle T \rangle$  and  $\langle T^2 \rangle$  denote  
131 the mean and the mean squared ISIs, respectively. Thus, a larger  $\lambda$   
132 corresponded to a stronger spiking coherence.

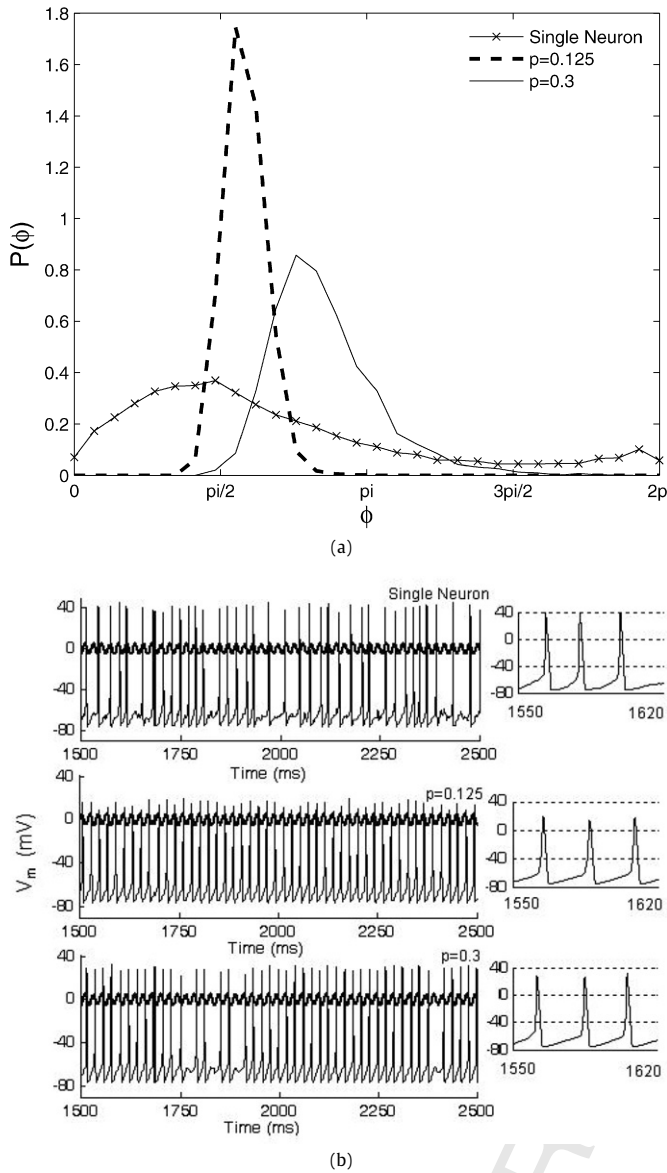


**Fig. 2.** Synchronization between the spiking activity and the subthreshold periodic stimulus for the network with two different values of  $p = 0.125$  and  $p = 0.3$ , and also for a single neuron at  $\omega = 0.3 \text{ ms}^{-1}$ : (a) the phase probability density of the spiking events versus phase of the stimulus, (b) the voltage trajectories ( $S = 6 \mu\text{m}^2$ ,  $\varepsilon = 0.1$ ). Inset: an example spike for each case ( $A = 1 \mu\text{A}/\text{cm}^2$ ).

### 3. Results

Gong et al. [14] investigated the effect of the network topology on the collective temporal coherence with fixed values for the cell area ( $S = 6 \mu\text{m}^2$ ), the angular frequency of the subthreshold periodic current ( $\omega = 0.3 \text{ ms}^{-1}$ ), and the coupling strength ( $\varepsilon = 0.1$ ) (Fig. 5 in [14]). To extend their findings, we first investigated how  $\lambda$  changes with the frequency of the forcing current. We computed  $\lambda$  of the network spike intervals during 100 second simulations, for twelve values of  $p$  ranging from 0.05 to 0.35, in each case for seven different frequencies ranging between 0.1–0.7  $\text{ms}^{-1}$  (Fig. 1). Consistent with the results of Gong et al. we found a clear ‘optimal island’ of  $\lambda$  in the  $\omega - p$  parameter space, around  $\omega \approx 0.3 \text{ ms}^{-1}$  and  $p \approx 0.125$ . We also found a second, smaller coherence peak for the same value of  $p$  but at  $\omega \approx 0.6 \text{ ms}^{-1}$ , thus the second harmonic of  $\omega \approx 0.3 \text{ ms}^{-1}$ .

To gain more insight in the dependence of coherence on  $p$ , and the role of the network versus the properties of the isolated neu-

ron, we then examined the synchronization between the network spiking and the subthreshold periodic stimulus for the optimal input frequency  $\omega \approx 0.3 \text{ ms}^{-1}$ . Following the approach used in [28, 30,31], we measured spike times from 1000 second simulations, modulo the stimulus period (in this case  $2\pi/\omega \approx 21 \text{ ms}$ ), to construct the phase probability density of the spike times,  $P(\phi)$ , for a single isolated neuron, and the network (thus the network spikes) with optimal ( $p = 0.125$ ) and sub-optimal ( $p = 0.3$ ) values of  $p$ . As shown in Fig. 2(a),  $P(\phi)$  has a very broad peak for a single neuron, whereas the network shows a more pronounced peak, or phase locking, for  $p = 0.3$ , and an even stronger phase locking for a value of  $p = 0.125$ .

In Fig. 2(b) we compare examples of the voltage trajectory for the single neuron simulation and the average voltage for the network, for the two values of  $p$  shown in Fig. 2(a). Compared to the precision of the network firing for  $p = 0.125$ , there is a weaker locking of the firing to the external stimulus for  $p = 0.3$ . As shown in Fig. 2(b), this frequency mismatch is even more pronounced for a single neuron. The insets of Fig. 2(b) show example waveforms over three cycles of the input, thus corresponding to full spikes in the single neuron case and averaged network spikes over all neurons in the network cases. As Gong et al. demonstrated [14], spatial synchronization across the network increases as  $p$  increases, and thus even though the temporal coherence over the entire response is greater for  $p = 0.125$ , the cycle-averaged network spikes have higher amplitudes for  $p = 0.3$  than for  $p = 0.125$ .

In order to provide more insight into the relationship between the spike timing and the stimulus, we obtained inter-spike interval histograms (ISIHs) computed from 10000 ISIs for a single neuron without external stimulus,  $I_{\text{ext}} = 0$ , and for the network spikes driven by an external subthreshold stimulus  $I_{\text{ext}} = \sin(0.3 \cdot t)$ , with the two values of  $p$  used above (Fig. 3). The ISIH of the single, un-driven neuron is very broad, with a distinct peak near the mean of the distribution (21 ms), corresponding to the period of subthreshold oscillations ( $\omega_{\text{osc}} \approx 0.3 \text{ ms}^{-1}$ ) [19], consistent with the frequency mismatch in the trace of Fig. 2(b). For the network with  $p = 0.125$ , the ISIH has a single sharp peak at the stimulus period, corresponding to a high degree of phase locking, i.e., a single dominant time scale in the spike trains [33]. In comparison, as suggested by the traces in Fig. 2(b), the network with  $p = 0.3$  has an ISIH with relatively wider multiple peaks at harmonics of the stimulus period, indicating lower phase locking and cycle skipping (reducing network output, i.e., the mean firing frequency), respectively.

To study the effects of the coupling strength on the network dynamics, we measured for different values of coupling strength over a range of  $p$  values, for both the un-driven case ( $I_{\text{ext}} = 0$ ) and the subthreshold driven case as before ( $I_{\text{ext}} = \sin(0.3 \cdot t)$ ). We arrived at three findings (Fig. 4). First, for any given coupling strength, the values of  $p$  that give the peak temporal coherence are the same, with or without subthreshold input. Second, at a given input condition, the peak value of  $\lambda$  as a function of  $p$  is similar for all coupling strengths. Third, in contrast, we found that coupling is inversely correlated with the value of  $p$  which gives the maximum  $\lambda$ . Thus, as coupling increases the peak  $\lambda$  is achieved for fewer added shortcuts (note the change in scale between Figs. 4(a), 4(b) and 4(c)).

Finally, we investigated how the network coherence depends on channel noise, first as a co-function of stimulus frequency and then as a co-function of  $p$ . Following the previous network simulations where a cell area of  $S = 6 \mu\text{m}^2$  showed the maximum coherence over all driving frequencies when  $p$  was equal to 0.125, we investigated how the coherence for this value of  $p$  changed with cell area ( $S = 0-50 \mu\text{m}^2$ ), and input frequency (0.1–0.7  $\text{ms}^{-1}$ ), for 100 second simulations of every network realization (Fig. 5). We found that coherence is strongly dependent on the cell area for all driving

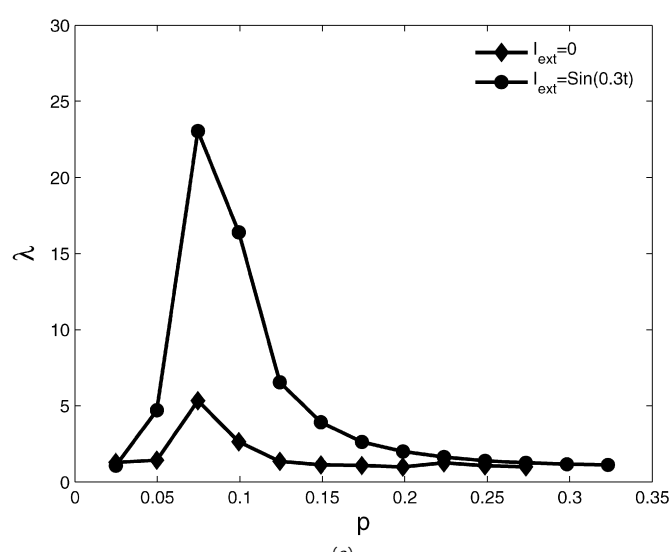
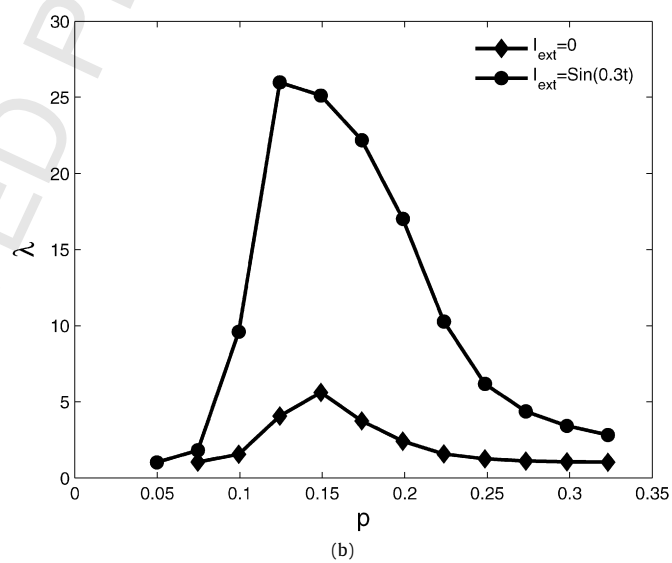
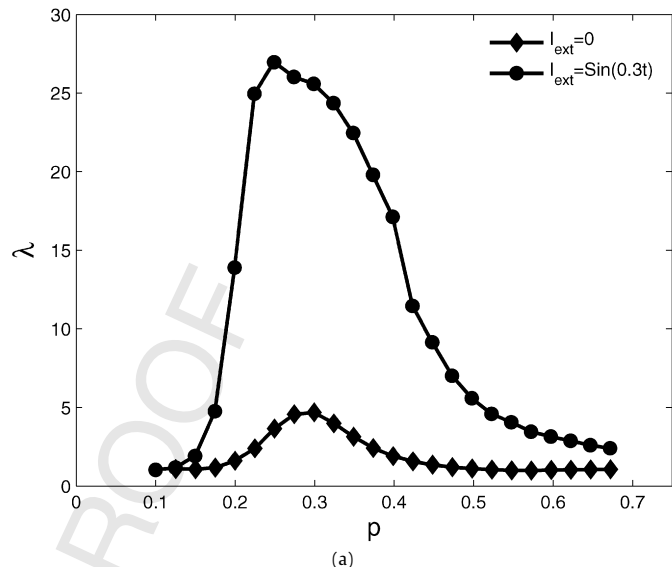
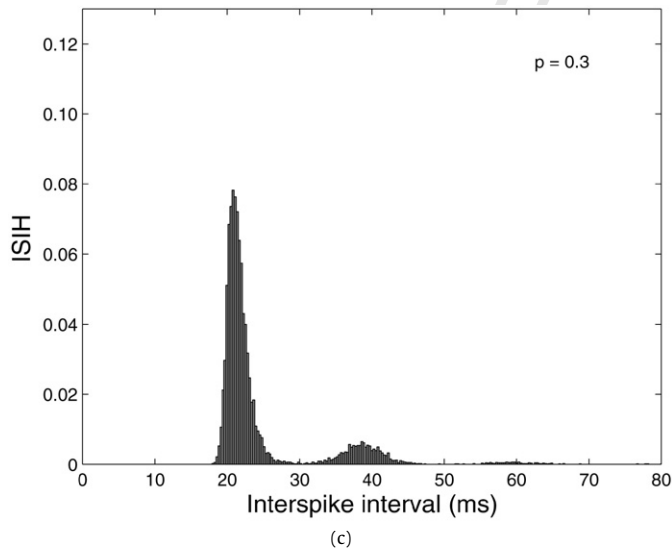
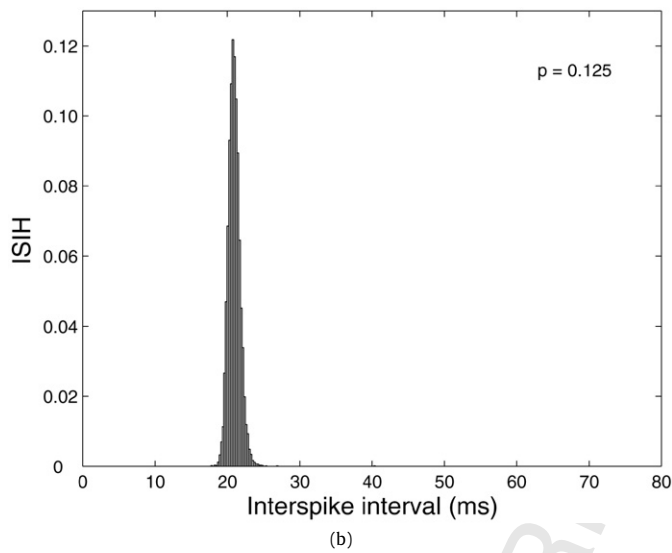
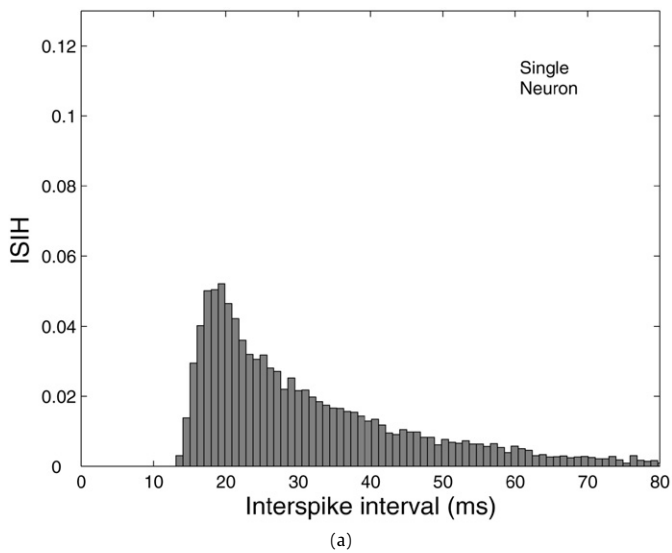
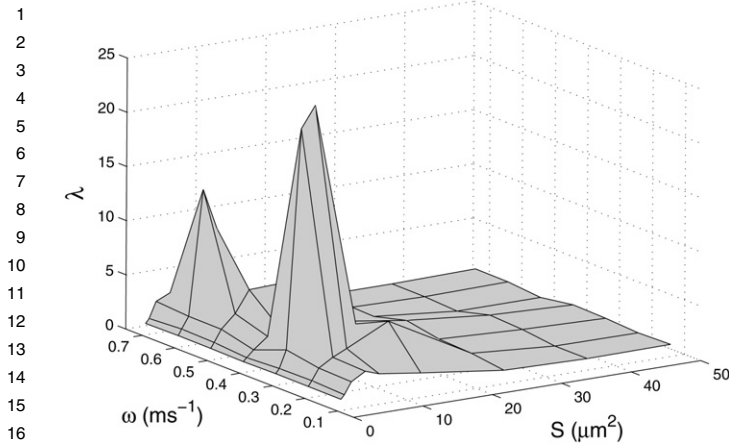


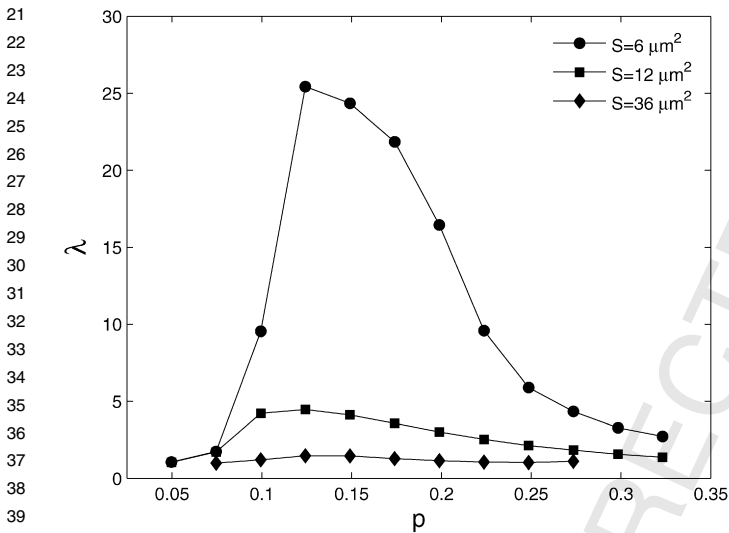
Fig. 3. The ISIHs calculated from 10 000 ISIs for (a) an undriven single neuron, and for the driven network with (b)  $p = 0.125$  and (c)  $p = 0.3$  ( $S = 6 \mu\text{m}^2$ ,  $\varepsilon = 0.1$ ,  $\omega = 0.3 \text{ ms}^{-1}$ ,  $A = 1 \mu\text{A}/\text{cm}^2$ ).

Fig. 4. Dependence of collective temporal coherence of the random network for the undriven case,  $I_{\text{ext}} = 0$ , and the driven case,  $I_{\text{ext}} = \sin(0.3 \cdot t)$  on the coupling strength: (a)  $\varepsilon = 0.05$ , (b)  $\varepsilon = 0.1$ , (c)  $\varepsilon = 0.2$ .





**Fig. 5.** Dependence of the best performance in the collective temporal coherence  $\lambda$  of the random network on the subthreshold stimulus frequency  $\omega$  and the cell membrane area  $S$  ( $p = 0.125$ ,  $\varepsilon = 0.1$ ,  $A = 1 \mu\text{A}/\text{cm}^2$ ).



**Fig. 6.** Dependence of collective temporal coherence  $\lambda$  of the random network on the membrane patch area  $S$  ( $\omega = 0.3 \text{ ms}^{-1}$ ,  $\varepsilon = 0.1$ ,  $A = 1 \mu\text{A}/\text{cm}^2$ ).

frequencies, with the best temporal coherence for small, but non-zero, cell areas, thus a specific range of intrinsic noise. We then re-examined the dependence of  $\lambda$  versus  $p$  at the optimal stimulation frequency of  $\omega = 0.3 \text{ ms}^{-1}$ , now for cell areas of 6, 12 and 36  $\mu\text{m}^2$  (Fig. 6). We found a resonance-like behavior of lambda with respect to  $p$  for the largest noise (thus,  $S = 6 \mu\text{m}^2$ ), which disappeared for smaller noise (thus, larger cells).

#### 4. Discussion

In this work we have extended the results by Gong et al. [14] describing the temporal coherence of complex SW networks of stochastic HH models driven by a subthreshold periodic stimulus. Specifically, we examined how the relationship between network topology and coherence is influenced by the frequency of the stimulus, by the coupling strength between neurons in the network and by the level of intrinsic noise in the neurons.

We found a distinct increase in coherence when both the frequency and the fraction of random shortcuts have optimal values ( $\omega \approx 0.3 \text{ ms}^{-1}$  and  $p \approx 0.125$ ), the same as Gong et al. [14]. The optimal frequency of  $\omega \approx 0.3 \text{ ms}^{-1}$  (or  $f \approx 50 \text{ Hz}$ ) corresponds to the frequency of intrinsic subthreshold oscillations for the HH neurons [19], suggesting that the network rhythmicity reflects a

direct coupling of oscillatory properties of the individual network elements [34,35]. We also found that stimuli close to the second harmonic of the intrinsic oscillations,  $\omega \approx 0.6 \text{ ms}^{-1}$ , gave a second, smaller peak in the temporal coherence. This result is consistent with the finding by Yu et al. [19] who described a small peak in the signal-to-noise ratio (SNR) for a globally coupled stochastic HH network near twice of the input frequency, due to the resonance between the signal and the second-order harmonic of the rhythmic oscillations. We also showed that an optimal level of the intrinsic channel noise obtains the best temporal coherence, and as the cellular noise decreases the network coherence decreases overall and becomes independent of  $p$ . By examining the phase probability density of the spike times,  $P(\phi)$ , and the ISIH we verified that increased network coherence is achieved by cells' firing during a narrower range of phases of the periodic stimulus, and that as coherence decreased, one to one cycle firing could be disrupted, leading to an overall reduction of the firing rate.

We obtained the dependence of network coherence on the probability of added shortcuts,  $p$ , for both the undriven and driven cases, for different coupling strengths, and showed that for each coupling strength the coherence has a maximum at around the same value of  $p$  for both the undriven and driven cases. This result indicates that resonator neurons exhibit coherence resonance (CR) [36–38] and stochastic resonance (SR) [39,40] for a robust optimal  $p$  in the absence and presence, respectively, of an external subthreshold signal, in the latter case especially when the frequencies of subthreshold oscillations and external stimulus match. We find that the value of  $p$  which gives the maximum coherence is lower for stronger coupling, showing an essential equivalence between the number of short cuts and the strength of the short cuts. This equivalence is not total, however, since for any level of coupling the coherence becomes very low for extreme values of  $p$  ( $p \rightarrow 0, 1$ ).

For a single neuron, previous work has shown that phase locking to a subthreshold periodic stimulus increases with decreasing noise intensity (equivalent to increasing the cell area for the stochastic HH model) [28,30,31], and shows an intrinsic coherence resonance with respect to noise [38,41]. Our results also demonstrate a similar resonance-like effect at the network level, where an optimal amount of noise in each cell leads to the maximum overall coherence. The dependence of coherence on topology and frequency (Fig. 1) and noise and frequency (Fig. 5) are roughly separable, suggesting a functional equivalence between topology and noise with respect to the network dynamics, at least in the subthreshold regime. This may be illustrated by the following analysis: For the single stochastic HH neuron model the optimal internal noise corresponds to a cell area around 1  $\mu\text{m}^2$ , whereas the optimal noise level for the network neurons that we describe is lower, corresponding to a cell area of around 4–6  $\mu\text{m}^2$ . Thus, topology serves in part as a scaling factor for intrinsic noise. Nevertheless, and similar to the relationship between coupling strength and topology, our results also demonstrate that cellular noise is necessary for there to be an influence of network topology on network coherence, and likewise that coherence only arises in the subthreshold regime for a constrained range of  $p$  values that describe the topology. Recently, Schmid et al. [42] provided an extension of a stochastic description of the HH model by including gating current effects, and showed that the resulting phenomenological fluctuations in capacitance partially compensate the effect of channel noise. As a future work, we plan to address the impact of the gating currents on the collective temporal coherence for the same network model.

The intrinsic resonance and resulting frequency preference of neurons, particularly relevant for small signals, have been suggested to serve as substrates for coordinating network activity in the brain [35]. The manner in which these properties are mani-

1 fested at the network level, particularly with respect to coherence  
 2 between neurons, and the dependence of their expression on con-  
 3 nectivity, may provide insights into the dynamics of coherent brain  
 4 activity. Our results suggest that for subthreshold inputs, network  
 5 topology has an influence on network activity mainly in the pres-  
 6 ence of large cellular noise: Noise provides an operating regime  
 7 that is specific for SW  $HH$  neural networks, being absent in regu-  
 8 lar and global networks, in which neurons exhibit strong coherence  
 9 in subthreshold signal encoding.

## 11 Acknowledgements

12 This work has been supported by a grant from The Scientific  
 13 and Technological Research Council of Turkey (TUBITAK), 219.01-  
 14 880-5768 to Dr. Mahmut Ozer, and a HFSP grant (RGP0049/2002)  
 15 and an Agence Nationale Recherche grant (FUNVISYNIN) to Dr.  
 16 Lyle J. Graham. The authors also thank Dr. Daniele Marinazzo for  
 17 his comments on the manuscript.

## 19 References

- 20 [1] S. Lawrence, C.L. Giles, *Science* 280 (1998) 98.  
 21 [2] R. Albert, H. Jeong, A.-L. Barabasi, *Nature* 401 (1999) 130.  
 22 [3] M.E.J. Newman, *Proc. Natl. Acad. Sci. USA* 98 (2001) 404.  
 23 [4] H. Jeong, S.P. Mason, A.-L. Barabasi, Z.N. Oltvai, *Nature* 411 (2001) 41.  
 24 [5] J. Camacho, R. Guimera, L.N. Amaral, *Phys. Rev. Lett.* 88 (2002) 228102.  
 25 [6] D.J. Watts, S.H. Strogatz, *Nature* 393 (1998) 440.  
 26 [7] M.E.J. Newman, D.J. Watts, *Phys. Lett. A* 263 (1999) 341.  
 27 [8] M.E.J. Newman, D.J. Watts, *Phys. Rev. E* 60 (1999) 7332.  
 28 [9] M.E.J. Newman, *J. Stat. Phys.* 101 (2000) 814.  
 29 [10] D.S. Basset, E. Bullmore, *The Neuroscientist* 12 (2006) 512.

- [11] L.F. Lago-Fernandez, R. Huerta, F. Corbacho, J.A. Siguenza, *Phys. Rev. Lett.* 84 (2000) 2758. 67  
 [12] O. Kwon, H.T. Moon, *Phys. Lett. A* 298 (2002) 319. 68  
 [13] D. Simard, L. Nadeau, H. Kröger, *Phys. Lett. A* 336 (2005) 8. 69  
 [14] Y. Gong, M. Wang, Z. Hou, H. Xin, *Chem. Phys. Chem.* 6 (2005) 1042. 70  
 [15] J.E. Levin, J.P. Miller, *Nature* 380 (1996) 165. 71  
 [16] W. Wang, Y. Wang, Z.D. Wang, *Phys. Rev. E* 57 (1998) 2527. 72  
 [17] F. Liu, J.F. Wang, W. Wang, *Phys. Rev. E* 59 (1999) 3453. 73  
 [18] F. Liu, J.F. Wang, W. Wang, *Phys. Lett. A* 256 (1999) 181. 74  
 [19] Y. Yu, W. Wang, J.F. Wang, F. Liu, *Phys. Rev. E* 63 (2001) 021907. 75  
 [20] A.L. Hodgkin, A.F. Huxley, *J. Physiol. (London)* 117 (1952) 500. 76  
 [21] E. Skaugen, L. Walloe, L. Acta Physiol. Scand. 107 (1979) 343. 77  
 [22] J.T. Rubinstein, *Biophys. J.* 68 (1995) 779. 78  
 [23] C.C. Chow, J.A. White, *Biophys. J.* 71 (1996) 3013. 79  
 [24] E. Schneidman, B. Freedman, I. Segev, *Neural Comput.* 10 (1998) 1679. 80  
 [25] J.A. White, J.T. Rubinstein, A.R. Kay, *Trends Neurosci.* 23 (2000) 131. 81  
 [26] M. Ozer, N.H. Ekmekci, *Phys. Lett. A* 338 (2005) 150. 82  
 [27] R.F. Fox, *Biophys. J.* 72 (1997) 2069. 83  
 [28] G. Schmid, I. Goychuk, P. Hanggi, *Physica A* 325 (2003) 165. 84  
 [29] G. Schmid, I. Goychuk, P. Hanggi, *Phys. Biol.* 1 (2004) 61. 85  
 [30] M. Ozer, *Phys. Lett. A* 354 (2006) 258. 86  
 [31] M. Ozer, M. Uzuntarla, S.N. Agaoglu, *Phys. Lett. A* 360 (2006) 135. 87  
 [32] M. Ozer, M. Uzuntarla, *Phys. Lett. A* 372 (2008) 4603. 88  
 [33] T. Verechtchaguina, I.M. Sokolov, L. Schimansky-Geier, *BioSystems* 89 (2007) 63. 89  
 [34] R. Llinas, *Science* 242 (1988) 1654. 90  
 [35] B. Hutcheon, Y. Yarom, *Trends Neurosci.* 23 (2000) 216. 91  
 [36] H. Gang, T. Ditzinger, C.Z. Ning, H. Haken, *Phys. Rev. Lett.* 71 (1993) 807. 92  
 [37] A.S. Pikovsky, J. Kurths, *Phys. Rev. Lett.* 78 (1997) 775. 93  
 [38] G. Schmid, I. Goychuk, P. Hanggi, *Europhys. Lett.* 56 (2001) 22. 94  
 [39] L. Gammaitoni, P. Hanggi, P. Jung, F. Marchesoni, *Rev. Mod. Phys.* 70 (1998) 223. 95  
 [40] D.F. Russel, L.A. Wilkens, F. Moss, *Nature* 402 (1999) 291. 96  
 [41] P. Jung, J.W. Shuai, *Europhys. Lett.* 56 (2001) 29. 97  
 [42] G. Schmid, I. Goychuk, P. Hanggi, *Phys. Biol.* 3 (2006) 248. 98  
 99  
 100  
 101  
 102  
 103  
 104  
 105  
 106  
 107  
 108  
 109  
 110  
 111  
 112  
 113  
 114  
 115  
 116  
 117  
 118  
 119  
 120  
 121  
 122  
 123  
 124  
 125  
 126  
 127  
 128  
 129  
 130  
 131  
 132